

Ossi Kimmelma, Matti Kaivola, Ilkka Tittonen, and Scott Buchter. 2007. Short pulse, high peak power, diode pumped, passively Q-switched 946 nm Nd:YAG laser. *Optics Communications*, volume 273, number 2, pages 496-499.

© 2006 Elsevier Science

Reprinted with permission from Elsevier.

# Short pulse, high peak power, diode pumped, passively Q-switched 946 nm Nd:YAG laser

Ossi Kimmelma<sup>a,\*</sup>, Matti Kaivola<sup>a</sup>, Ilkka Tittonen<sup>a</sup>, Scott Buchter<sup>b,a</sup>

<sup>a</sup> *Optics and Molecular Materials and Center for New Materials, Helsinki University of Technology, Micronova, P.O. Box 3500, FI-02015 TKK, Finland*

<sup>b</sup> *Arctic Photonics, Sinikalliontie 4, FI-02630 Espoo, Finland*

Received 20 October 2006; accepted 12 January 2007

## Abstract

We report on generation of 946 nm laser pulses of a few nanosecond duration and up to 3.7 kW peak power from a compact diode-pumped passively Q-switched Nd:YAG laser. This power is 2.5 times as much as what previously has been obtained from this type of a laser. The short pulses with the record high peak power may be particularly attractive for laser range finding type applications.  
© 2006 Elsevier B.V. All rights reserved.

*PACS:* 42.55.Xi; 42.60.Gd

*Keywords:* Solid-state lasers; Passively Q-switched lasers; Quasi-three-level lasers

## 1. Introduction

Diode-pumped passively Q-switched solid-state lasers offer a simple and efficient means to produce high peak power laser pulses in the nanosecond region. Recently, the quasi-three-level laser schemes in rare-earth-ion doped materials have received special attention in this context, since several quasi-three-level transitions enable efficient generation of blue laser light by frequency doubling the output of the Q-switched laser. Blue light generation, however, is not the only attraction offered by these lasers. For the case of Nd ion, the wavelength of the quasi-three-level laser operating on the  ${}^4F_{3/2} \rightarrow {}^4I_{9/2}$  transition is in the range of 900–950 nm depending on the host crystal. This is clearly shorter than the wavelength of 1064 nm that the traditional four-level Nd-lasers operate on. The shorter wavelength may give a clear advantage in applications depending critically on the detector sensitivity which, for

instance, for the widely used and cost-effective silicon detectors peaks at around 900 nm, and has a steep drop towards the wavelength corresponding to the bandgap for silicon at 1.1  $\mu\text{m}$ .

The first report on a passively Q-switched Nd:YAG laser operating at 946 nm is by Liu et al. who used a monolithic Cr–Nd:YAG construction [1]. Later, an average power as high as 2.1 W at 946 nm has been achieved by using a co-doped Nd–Cr:YAG crystal [2]. In another approach, up to 80  $\mu\text{J}$  energies in pulses of 80 ns duration have been obtained in a similar kind of system [3].

In this work, we report on the construction of a compact, diode-pumped 946 nm Nd:YAG laser that is passively Q-switched with a Cr:YAG crystal. The laser puts out 5–7 ns pulses with up to 3.7 kW peak power which is ca. 2.5 times as much as what previously has been obtained from this type of a laser [1]. The laser could be an ideal source for, e.g., laser range finding applications, where the short pulse duration, high peak power, excellent beam quality, and short output wavelength can be combined to facilitate good spatial resolution, long operation range and high detection sensitivity for the system.

\* Corresponding author. Tel.: +358 405046948.

E-mail address: [Ossi.Kimmelma@tkk.fi](mailto:Ossi.Kimmelma@tkk.fi) (O. Kimmelma).

## 2. Setup

The general layout of the laser is depicted in Fig. 1. The pump power is provided by a fiber coupled laser diode emitting at 808 nm. The diameter of the pump fiber is 100  $\mu\text{m}$  with a numerical aperture of 0.22. The output from the fiber is collimated and focused onto the laser crystal with a pair of aspheric lenses with focal lengths of 7.5 mm and 13.8 mm. These values were selected to give a 92  $\mu\text{m}$  pump radius in the 1.5 mm long laser crystal whose transverse dimensions are  $5 \times 5 \text{ mm}^2$ . The rear surface of the crystal has a dielectric coating which is highly reflective at 946 nm and highly transmissive at 808 nm and 1064 nm. The laser cavity is formed between the coated rear surface of the crystal and a spherical dielectric mirror which is placed on a translation stage to allow for convenient tuning of the cavity length. The radius of curvature and reflectivity of the output coupler is 150 mm and 92%, respectively. It is essential that the cavity ends are highly transmissive at 1064 nm to prevent parasitic laser oscillation in this high-gain transition and that the front surface of the laser crystal is anti-reflection (AR) coated at the laser wavelength in order to eliminate formation of secondary cavities.

The laser crystal is doped with 1% of Nd which leads to 57% of the pump power to be absorbed in the 1.5 mm long crystal. Efficient cooling of the active material is facilitated by circulating water through the crystal mount made of copper. Passive Q-switching of the laser is obtained by placing a 0.3 mm thick  $\text{Cr}^{4+}$ :YAG crystal with AR-coated surfaces in between the laser crystal and the output coupler. The unsaturated transmission of the Cr-crystal is 95%.

Selection of the reflectivity of the output coupler is a trade-off between obtaining short pulses, high pulse energy and low lasing threshold. The reflectivity and curvature of the mirror also affect on the intracavity intensity which needs to stay below the damage threshold of the coatings. A broad transverse area of the lasing mode is desired in order to maximize the energy extraction while a short cavity is required for short output pulses. For a simple nonplanar two-mirror cavity these conditions are mutually exclusive. Physical phenomena that additionally modify the laser output beam properties are aperture guiding [4] and thermal lensing. These effects change the transverse area of the laser mode as a function of the pumping power and the beam size of the pumping laser. In Nd:YAG, the

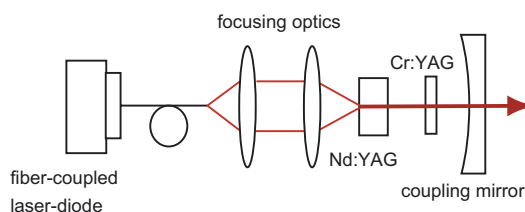


Fig. 1. Schematic picture of the setup.

created thermal lens is positive. Thus it decreases the beam radius in a short cavity.

The laser crystal has absorption at the lasing wavelength due to the thermally populated lower laser level. This population can, however, be reduced by intense pumping which empties the initially populated lower level. This results in formation of a high gain region in the center of the pump beam and absorption further away from the center, thus generating a soft aperture into the laser crystal. Usually, good mode matching between the pump beam and the lasing mode is desired in order to achieve high efficiency and low lasing threshold. In this work the goal was, however, to maximize the area of the lasing mode with the given pulse length. A narrow pump beam creates a small soft aperture and a strong thermal lens which will decrease the laser mode size. A bigger pump spot enables a larger transverse lasing mode area resulting in higher pulse energy, but with somewhat lower efficiency and higher lasing threshold. Our tests with a pump spot size comparable to the size of the lasing mode gave a good efficiency in CW operation but a lower peak power in the pulsed mode. The laser crystal length was chosen to be 1.5 mm in order to ensure bleaching of the whole lasing volume with the pump laser. Attempts to further increase the peak power by replacing the Q-switch crystal with one having a lower unsaturated transmission of 90% resulted in damaging of the coatings.

## 3. Results

With a 9 mm optical length of the cavity, the laser generates pulses that are 6.3 ns long (FWHM), have an average power of 216 mW and a pulse energy of 23  $\mu\text{J}$ . This corresponds to a peak power of 3.7 kW. A power of 2.6 W was absorbed in the laser crystal, out of an incoming pump power of 4.6 W. The short term stabilities of the pulse width, the period between the pulses and the peak power were 2%, 3% and 4%, respectively. The mode was Gaussian  $\text{TEM}_{00}$ . An oscilloscope trace of the temporal profile of the laser pulse is shown in Fig. 2.

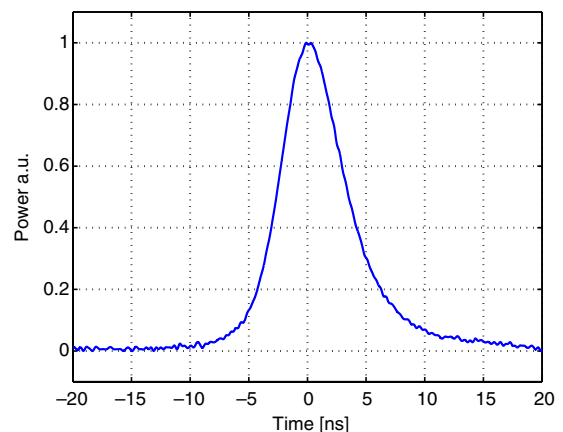


Fig. 2. An oscilloscope trace of a single 946 nm laser pulse.

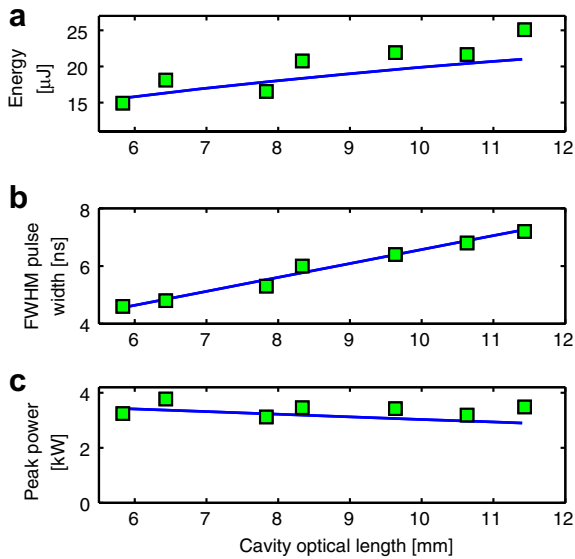


Fig. 3. Pulse parameters as a function of the optical length of the cavity: (a) measured (squares) and calculated values (line) for pulse energy, (b) measured values (squares) and fitted line for pulse length (FWHM) and (c) peak power calculated from data of Figures (a) and (b).

We performed a series of measurements to investigate the dependence of the pulse parameters on the resonator length. The measurement results for the pulse energy, pulse width (FWHM) and the resulting peak power are presented as a function of the optical length of the resonator in Fig. 3. The measured values are marked with squares. The solid line in Fig. 3a presents the calculated pulse energy values obtained by using the model of Patel et al. [5]. Within this model, the output energy of a passively Q-switched laser is given as a solution to a transcendental equation derived from the laser rate equations that include the effects of the excited-state absorption in the saturable absorber. The output energy is obtained in terms of known spectroscopic and easily accessible cavity parameter values. The laser mode size, appearing in the calculation, was evaluated with a Gaussian beam propagation method including the effects of thermal lensing [6,7] and formation of the soft aperture [4]. The pump beam size was used as the size for the soft aperture. As can be seen, the values of the measured and calculated pulse energies are in good agreement. The parameter values that were used in the calculations, are listed in Table 1. The line appearing in the pulse length graph of Fig. 3b represents a linear fit to the measurement results. Solid line in the Fig. 3c represents an estimate for the peak power and it is obtained as a ratio of the calculated pulse energy to the fitted pulse length values.

In the measurements, the Q-switch crystal was kept at a fixed position relative to the laser crystal in order to minimize the spatial variation in the operation of the saturable absorber. When changing the cavity length by moving the output coupler, the laser required a slight readjustment of its alignment. In this process, the average output power was maximized so that no after pulses appeared with a

Table 1

Laser and saturable absorber (SA) parameters used for calculation		
Parameter	Value	Reference
Spectroscopic emission cross section for laser	$2.8 \times 10^{-20} \text{ cm}^2$	[8]
One way cavity transmission exclusive of ground-state laser ion absorption and SA loss	0.992	
Lower level Boltzmann thermal population	0.6	[6]
Upper level Boltzmann thermal population	0.0074	[6]
Upper state lifetime	230 $\mu\text{s}$	[6]
SA cross section at the excited state	$4 \times 10^{-19} \text{ cm}^2$	[9]
SA cross section at the ground state	$1.1 \times 10^{-18} \text{ cm}^2$	[9]
Thermal conductivity	0.14 W/cm/K	[6]
Fractional thermal loading	0.15	[6]
$dn/dt$	$7.3 \times 10^{-6} \text{ 1/K}$	[6]
Thermal expansion	$7.4 \times 10^{-6} \text{ K}^{-1}$	[6]
Poisson's ratio	0.25	[10]

pump power of 4.5 W (the absorbed power was 2.5 W). The average output power was between 98 mW and 147 mW when the laser was operating stably in TEM<sub>00</sub>-mode. The beam was observed with a beam camera at the focus of a lens. The observation of the transverse beam in  $x$  and  $y$ -directions show very good match to Gaussian profile. The beam profiles can be seen in Fig. 4.

The measurement results are in good agreement with the theoretical calculations. The peak power was observed to vary only slightly over the measured cavity length range making it possible to choose the desired pulse length and energy by changing the cavity length during which there is only minor variation in the peak power.

Two things happen when the cavity is shortened; the mode gets smaller and the pulse becomes shorter as the res-

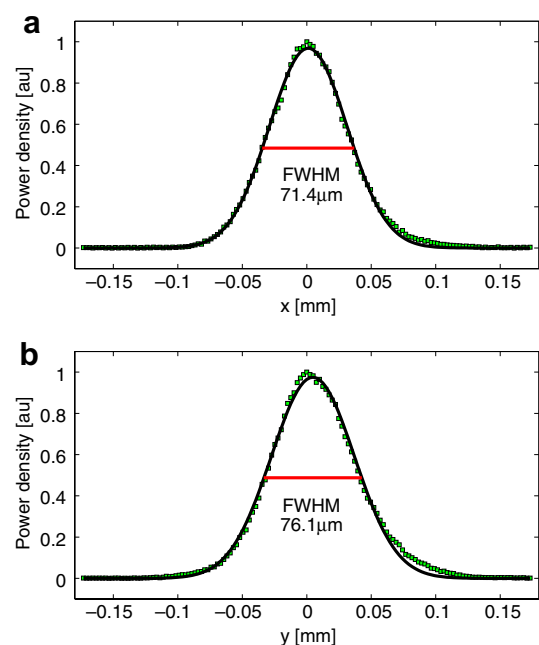


Fig. 4. Beam profiler measurement of the focused beam in  $x$  and  $y$ -directions (squares), Gaussian fit to the data (lines) and FWHM width.

onator photon lifetime gets shorter. The latter effect is in general more effective and the peak power should rise as the resonator length is shortened. The peak intensity inside our resonator is  $570 \text{ MW/cm}^2$  with the approximated beam radius of  $100 \mu\text{m}$  at the Cr:YAG crystal. This already exceeds the damage threshold of the coatings,  $500 \text{ MW/cm}^2$ , limiting the peak power of the laser output approximately to the level that was measured. This explains why no significant improvement to the peak power in the presented setup was possible by further shortening the laser cavity. The imminent damage threshold became evident as the measurements were carried out.

#### 4. Conclusions

We have produced high peak power pulses at  $946 \text{ nm}$  using a passively Q-switched Nd:YAG laser pumped by a fiber-coupled laser diode at  $808 \text{ nm}$ . The achieved peak power was  $3.7 \text{ kW}$  with a pulse energy of  $23 \mu\text{J}$  and FWHM pulse length of  $6.3 \text{ ns}$ . The average power was  $216 \text{ mW}$ . The laser properties are well suited, e.g. for the needs of laser range finding. The simple construction together with the high peak power also offer a good starting point for use of the laser as a pump source for fre-

quency conversion applications, in particular for obtaining blue light through second harmonic generation.

#### Acknowledgements

This work was supported by the Graduate School of Electrical and Communications Engineering, the Finnish Foundation of Technology and the Finnish Academy of Science and Letters.

#### References

- [1] H. Liu, O. Hornia, Y.C. Chen, S. Zhou, IEEE J. Sel. Top. Quantum Electron. 3 (1997) 26.
- [2] L. Zhang, C.Y. Li, B.H. Feng, Z.Y. Wei, D.H. Li, P.M. Fu, Z.G. Zhang, Chin. Phys. Lett. 22 (2005) 1420.
- [3] T. Kellner, G. Huber, S. Kück, Appl. Opt. 37 (1998) 7076.
- [4] T.Y. Fan, Opt. Lett. 19 (1994) 554.
- [5] G.D. Patel, R.J. Beach, IEEE J. Quantum Electron. 37 (2001) 707.
- [6] W. Koechner, Solid-State Laser Engineering, Springer, New York, 1999.
- [7] S.C. Tidwell, J.F. Seamans, M.S. Bowers, A.K. Cousins, IEEE J. Quantum Electron. 28 (1992) 997.
- [8] C.W. Wang, Y.L. Weng, P.L. Huang, H.Z. Cheng, S.L. Huang, Appl. Opt. 41 (2002) 1075.
- [9] X. Zhang, A. Brenier, J. Wang, H. Zhang, Opt. Mater. 26 (2004) 293.
- [10] D.C. Brown, IEEE J. Quantum Electron. 33 (1997) 861.